Ferroelectrics, 1994, Vol. 155, pp. 377–382
Reprints available directly from the publisher
Photocopying permitted by license only

EFFECT OF "GUEST" MOLECULES SUBSYSTEM DIMENSION ON PHASE TRANSITIONS AND INCOMMENSURATE STATES IN GRAPHITE INTERCALATION COMPOUNDS $C_{5n}HNO_3$

(Received August 9, 1993)

ALBERT M. ZIATDINOV, NIKOLAY M. MISHCHENKO
Institute of Chemistry, Russian Academy of Sciences,
690022 Vladivostok-22, Russia

Abstract In graphite intercalation compounds (GICs) $C_{5n}HNO_3$ (n = 2, 4) the unknown succession of phase transitions, change of quantity and mobility of spin carriers in compounds of different stages (with different intercalate subsystem dimension) and at intercalate crystallization (T<250 K) has been found and investigated by means of conduction carriers electron spin resonance (ESR) at X- and Q- band frequency.

INTRODUCTION

Graphite intercalation compounds (GICs) consist of an alternating sequence of n hexagonal graphite monolayers (n is the stage) and a monolayer of foreign atoms or molecules (intercalate).[1] For small n (= 1, 2, sometimes 3) the intercalate subsystem is three-dimensionally (3-D) ordered. The ordering of an intercalate subsystem along the **c**-axis of graphite (3-D) disappears as the n increases (usually, beginning with n > 3). The ability to vary the strength of interlayer interactions in GICs at the synthetic level suggests the possibility of systematically investigating phenomena unique to this compounds such as the dependence of behaviour of phase transitions in intercalate layers (e.g. melting) on intercalate subsystem dimensions (i.e. on the n). Particularly, in GICs with nitric acid, $C_{5n}HNO_3$ (n = 1, 2,..), a liquid-like subsystem of HNO_3 molecules lower $T_c \cong 250$ K are ordered and form a crystal which for n = 2(4) is incommensurable (commensurable) with a carbon net along one of its crystallographic directions.[2-4] Therefore, this compounds excite special interest as objects suitable for studing various problems of physics of low-dimensional systems, especially of crystallization (melting) of intercalate layers in periodic external potential and its dependence on stage index.

In this report we give the results of the conduction carrier ESR-investigation in GIC $C_{5n}HNO_3$ (n = 2 and 4) of the effect of the HNO_3 molecules subsystem dimension on the intercalate layer crystallyzation (melting) and the new phenomenon which takes place at the lattice liquid crystallization and does not occur in the 3-D HNO_3.

EXPERIMENTAL PROCEDURE

Synthesis of GICs $C_{5n}HNO_3$ (n = 2, 4) for ESR - studies was carried out on higly oriented pyrolitic graphite (HOPG) plates with different width (l), height (h) and thickness (d), where lxd is the square of a side of a sample perpendicular to the c-axis. Two different series of samples were synthesized as for the 2-nd and 4-th stage compounds. In the first series for n = 2(4), l changed in the interval 0.05÷0.225 (0.04÷0.22) cm at constant h = 0.5 (0.5) cm and d = 0.01 (0.018) cm. In other series d changed for n = 2(4) in the interval 0.1÷0.34 (0.2÷0.4) cm at constant h = 0.5 (0.5) cm and l= 0.225 (0.32) cm. Accuracy of the plates sizes determination was $\sim 5 \cdot 10^{-3}$ cm. Samples with n = 2 and n = 4 were synthesized in "steaming" nitric acid with density ρ = □ 1.565 g/cm³ and in dilute nitric acid with ρ = 1.48 g/cm³, respectively. The GIC stage was controlled by diffraction method. According to data of contactless basal plane resistivity measurements of 2-nd (4-th) stage GIC plates at ~300 K $\sigma_a \simeq 1.5\ (3,2) \cdot 10^5$ ohm^{-1}·cm^{-1}. According to literature data[5] for 2-nd stage compounds at 300 K $\sigma_c \cong 2$ ohm^{-1}·cm^{-1}.

ESR measurements in X(Q) band were conducted in the rectangular (cylindrical) resonator with mode TE_{102} (H_{011}) at 2.5 (100) kHz modulation and at T=100÷300 K. In the rectangular resonator, the structure of the electromagnetic field of the TE_{102} mode has such a form that at a conventional setting of resonator a constant magnetic field H is parallel to the electrical component $\tilde{E}$ of the microwave field (MWF). GIC plates were placed in the resonator in such a way that basic and two lateral sides (hxd) were parallel to the magnetic component ($\tilde{H}$) of the MWF. In area T_c temperature changed gradually with a step $\Delta T \simeq 0.2$ K and was kept up with accuracy $\simeq$ 0.1 K/hour.

RESULTS

The single ESR signal of $C_{10}HNO_3$ with axial angular dependence relative to the c-axis and $g_{\parallel} = 2.0023 \pm 0.0002$ and $g_{\perp} = 2.0028 \pm 0.0002$ is observed in both GIC phases from

all plates. At $T < T_c^-$ lineshapes have a "normal" phase - in the sense that peak A is situated in smaller magnetic fields relative to peak B and A/B (1) curve has one gentle sloping maximum at l_m = 0.1 cm (Figure 1B). At $T > T_c^+$, A/B(1) dependence has a four peaked shape (Figure 1A). At $\theta \approx 90^\circ$ (θ - angle between c--axis and **H**) the A/B(1) maximum is observed at l_m = 0.10, 0.12, 0.14 and 0.17 cm. Plates with l_m have a lineshape symmetrical relative to peak A. For plates with l from three adjoining areas between l_m, peak A of the line situated in larger magnetic fields in comparison with peak B (a "reversed" phase).

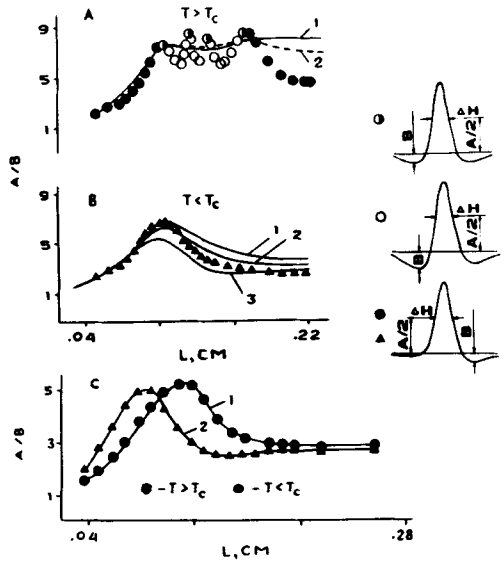

The ESR signal of $C_{20}HNO_3$ has the same direction of the axial axis and values of g-tensor as the 2 -nd stage sample. For all sizes of samples and temperatures the lineshapes have a "normal" phase. At $T > T_c^+$ ($< T_c^-$) the A/B (1) curve has one gentle sloping maximum at l_m= 0.12 (0.09) cm (Fi-

FIGURE 1 The experimental and the theoretical values of the line-asymmetry ratio A/B for the ESR derivative spectra of $C_{10}HNO_3$ (A, B) and $C_{20}HNO_3$ (C) as a function of the sample width (l). A: the solid line is the Dyson's theoretical curve for $R \approx (T_D/T_2)^{1/2} = 0.1$, the dashed line is calculated for R = 0.1, taking into account the additional absorption of the MWF, with A/B =1, 3 % peak intensity and the same line width as the delocalized spins spectrum Half-dark and light points correspond to a simmetrical line and to a 'reversed' phase, line respectively. B: curve 1(3) corresponds to the Dyson's theoretical curve for R = 0.8 (1.5); curve 2 is calculated as the dashed curve in A, but with R= 0.9; d = 0.01 cm, h = 0.5 cm. C: curve 1(2) corresponds to the Dyson's theoretical curve for R= 1.2 (2.0); d = 0.018 cm, h = 0.5 cm. $\mathbf{H} \perp \mathbf{c}$, X-band.

gure C). In both stages of the GIC at $l \rightarrow 0$ the lineshapes tend to Lorentzian and at constant l and h, A/B of the lineshapes do not depend on d.

The regime of passage of phase transition was choosen based on the studies of temperature dependence of time $\Delta\tau(T)$ from the moment of gradual variation of temperature on ΔT to saturation of peak intensity of the ESR signal. At cooling (heating) of 2-nd stage samples at T_c^+ (T_c^-)=250(253) ± 0.5 K, the dependence $\Delta\tau(T)$ has a clear maximum (Figure 3). This temperature was taken as phase transition temperature in $C_{10}HNO_3$, later on.

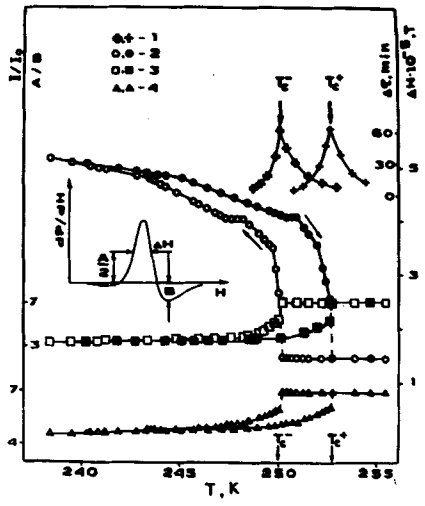

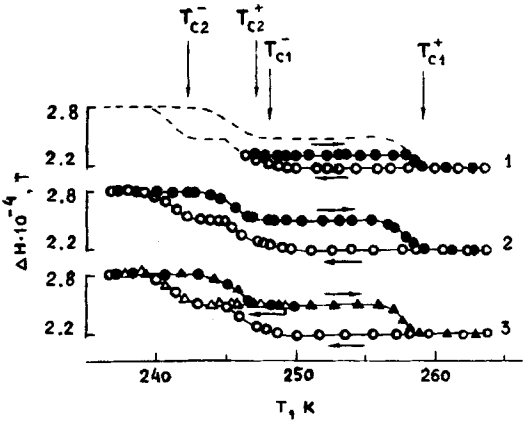

FIGURE 2 $\Delta\tau(1)$ and parameters of the ESR line of $C_{10}HNO_3$, i.e., ΔH (2), A/B(3) and $I/I_o(4)$ (I_o -intensity of a standard signal) as a function of temperature. d = 0.01 cm, h = 0.5 cm, l = 0.18 cm. X-band.

FIGURE 3 The ESR line width ΔH of the $C_{20}HNO_3$ as a function of temperature for different case of passing from the liquid to the solid phase of HNO_3. X-band.

At $T > T_c^+$, the width (ΔH), the integral intensity $I = (A + B)\cdot\Delta H^2$ and A/B of ESR lines for n = 2 and 4 do not depend on temperature. For n = 2 at T_c all parameters of the line undergo sharp, nearly step-wise changes (Figure 2). In the crystal phase of the intercalate, ΔH (I) increases (decreases) as temperature decreases. Simultaneously, the A/B of the samples with l=0.18 (l>0.22) cm for n=2, decreases to 3.4 ± 0.1 (3.0 ± 0.2) at saturation obtained

at T≃100 K. Curve ΔH(T) for n=2 in the interval T_c^--10 K < < T < T_c^- has a peculiarity: it consists of several linear sections with different slopes. One of them observed at (T_c^- - 2.7)K <T< (T_c^- - 1.9)K is parallel to the abscissa axis. It is interesting to note, that the curve for n = 4 also contains the parallel section corresponding to the abscissa axis, which is situated between two inclined parts (Figure 3). Integral intensities of signals also do not change in this intervals of temperature. At temperature increase, parameter values of ESR line change in a reverse consequence, but with a "global" temperature hysteresis (Figure 2 and 3). Transitions between corresponding linear sections of ΔH(T) curve take place for both stages at the same parameter values of the line, independently of a direction of temperature variation. At powers of MWF field far from saturation and at the same temperature, ΔH values in Q-band ≃15 % more than that in X-band.

DISCUSSION.

In $C_{10}HNO_3$ multipeaked shape of the A/B(l) curve with areas of "reversed" phase of the line shape with A/B >2.55 at large l (Figure 1A) testifies high mobility of spin carriers at T > T_c^+[8] and, vice versa, the single-peaked A/B(l) dependence, with A/B ≃ 3 at large l (Figure 1B) is typical for weak diffusion spins in metals.[8] Similar, from Figure C, it can be concluded, that in both phases of 4 - th stage GIC only weak diffusion spins are present. The independence of g-tensor values of spin carriers at changes of agregate states of intercalate and their closeness to the g-factor of the free electrons testify that the density of their probability on intercalate molecules is small and does not change at phase transition. A very weak frequency dependence of ΔH indicates that its growth at lower T_c^- is not due to increase of degree of axis scattering and (or) values of g - tensor. Comparision of the Figure 2 and 3 indicates that the values and character of variations of ΔH curves essentially depend on stage index, i.e., on the dimension of intercalate sublattice. However, it is of interest that at intercalate crystallization the full values of ΔH increasing are the same in both stages. By assuming that the centres of perturbation of conduction electron spin wave functions are situated preferencely at the edges of the Dumas - Herold islands,[7] the mentioned independence of ΔH value increasing at T_c on stage index and the fact of observation of larger values of ΔH for compounds with larger stage index can be put down to increasing the number

and decreasing the size of Dumas - Herold islands in GICs with large stage index. In particular, NO_3^- - ions and p_z-radicals can serve as perturbation centres.

At $T > T_c$ ($<T_c$), for all plates, the conduction carrier ESR lineshape of $C_{20}HNO_3$ is described by the standard one-dimensional Dyson's formula[8] for the conduction plates of the finite dimension involving $\sigma_c \cong 1.63(2.90)$ ohm^{-1}.cm^{-1}, T_D (diffusion time of a spin across the skin depth δ_c, which will be governed by σ_c) $= 4.0 \cdot 10^{-8}$ ($8.4 \cdot 10^{-8}$) sec and T_2 (spin-lattice relaxation time) $= 2,8 \cdot 10^{-8}$ ($2,1 \cdot 10^{-8}$) sec (Figure 1C). The σ_c value was estimated from relation $l_m/\delta_c = 2,85$,[8] where l_m is the coordinate of the A/B (1) curve maximum. The T_D and T_2 parameters values were determened by the standard Feher-Kip procedure.[10] Thus, at a phase transition T_D increases by 2 - fold. Simultaneously, σ_a of the $C_{20}HNO_3$ plates increases by $\simeq 20$ %.[11] In terms of a GICs rigid band model,[1] the latter two results indicate, together, that at the crystallization of the intercalate, the electron density passes to the intercalate layers from the graphite layers.

In $C_{10}HNO_3$, even for the quality explanation of the A/B (1) curve, the presence of an additional MWF absorbtion depending on 1 requires to assume (Figure 1, A and B). A detailed treatment of the nature of this absorbtion will be published elsewhere.

REFERENCES

1. M. S. Dresselhaus and G. Dresselhaus, Adv. in Phys., 30, 139(1981).
2. H. J. Samuelseen, R. Moret, H. Fuzellier, M. Klatt, M. Lelaurain and A.Herold, Phys. Rev., B32,417(1985).
3. R.Clark, P.Hernandez, H.Homma and E. Montague, Synth. Met., 12, 27(1985).
4. M. J. Bottomley, G.S. Parry and A.R. Ubbelohde, Proc. Roy. Soc. London, A297, 291(1964).
5. A. R. Ubbelohde, Proc. Roy. Soc. London, A231, 445 (1972).
6. H. J. Kodera, Phys. Soc. Jpn, 28, 89(1970).
7. N.Dumas and Herold, C.R. Seances, Acad. Sci., C268, 373(1969).
8. F. J. Dyson, Phys. Rev., 98, 349(1955).
9. Pifer J.H., Magno R., Phys. Rev., B3, 663(1971).
10. Feher G., Kip A.F., Phys. Rev., 98, 337(1955).
11. Solin S. A., Adv. Chem. Phys., 49, 455(1982).